First evidence of active transpressive surface faulting at the front of the eastern Southern Alps, northeastern Italy. Insight on the 1511 earthquake seismotectonics

Emanuela Falcucci[1], Maria Eliana Poli[2], Fabrizio Galadini[1], Giancarlo Scardia[3] Giovanni Paiero[2]
5   Adriano Zanferrari[2]

[1]Istituto Nazionale di Geofisica e Vulcanologia, Roma, Via di Vigna Murata 605, 00143, Italy
[2] University of Udine – Dept. of Agricultural, Food, Environmental and Animal Sciences, Udine, Italy.
[3] Universidade Estadual Paulista (UNESP), Instituto de Geociências e Ciências Exatas, Rio Claro – SP, Brazil.

10   *Correspondence to*: Emanuela Falcucci (emanuela.falcucci@ingv.it)

Abstract. We investigated the eastern corner of northeastern Italy, where the NW-SE trending dextral strike-slip fault systems of western Slovenia intersects the south-verging fold and thrust belt of the eastern Southern Alps . The area suffered the largest earthquakes of the region, among which are the 1511 (Mw 6.3) event and the two major shocks of the 1976 seismic sequence, with Mw=6.4 and 6.1 respectively. The Colle Villano thrust and the Borgo Faris-Cividale strike-slip fault
15   have been first analyzed by interpreting industrial seismic lines and then by performing morpho-tectonic and paleoseismological analyses. These different datasets indicate that the two structures define an active, coherent transpressive fault system that activated twice in the past two millennia, with the last event occurring around the 15th-17th century. The chronological information, and the location of the investigated fault system suggest its activation during the 1511 earthquake.

20   **Keywords.** active transpressive surface faulting, paleoseismological investigations, 1511 earthquake, eastern Southern Alps.

1 Introduction

The Late Miocene-Quaternary counterclockwise rotation and contemporaneous northward drift of the Adria microplate indenter resulted in the development of the eastern Southern Alps, which are connected to the Dinarides towards the east. The Adria microplate kinematics determined diffuse dextral strike-slip deformation in Slovenia and prevailing thrusting at
25   the eastern Southern Alps, in northeastern Italy (Zanferrari et al., 2013). Seismicity reflects such a kinematic transition, being characterized both by earthquakes caused by dextral strike-slip and inverse ruptures (Kastelic et al., 2008). This issue is by all means relevant considering that this region has been the focus of some of the strongest historical earthquakes of continental Europe, among which are the 1348 (Mw 6.6) and the 1511 (Mw 6.3) events, as well as the two major shocks of

the 1976 seismic sequence (Mw 6.4 and 6.1). In particular, despite the large number of studies (e.g., Ambraseys, 1976; Ribaric, 1979; Bavec et al., 2013), the epicentre, the causative fault(s) and the kinematics of the 1511 earthquake are still a matter of debate. Here we describe the results of a multi-disciplinary study performed in the 1511 earthquake area, based on geological-morphological surveys, industrial seismic lines interpretation, paleoseismological trenching and the drilling of a

5   20 m-deep core. Specifically, we focus on the Borgo Faris-Cividale Fault (henceforth BFCF), a dextral strike-slip structure that experienced a complex kinematic history (e.g., Zanferrari et al., 2008; Zanferrari et al., 2013), and the Colle Villano Thrust (henceforth CVT), that shows geomorphic hints of recent activity (Galadini et al., 2005). We aimed to understand the relationship between these very close structures and their role in the regional structural-kinematics framework, and to acquire new clues on the 1511 earthquake seismotectonics.

10 **2 Tectonic setting and seismic activity**

Since the Middle Miocene, the SSE-verging and WSW-ENE-trending fronts of the eastern Southern Alps in the Friuli region (Fig. 1a) (e.g., Castellarin et al., 2006, and reference therein) cut and re-folded the external Paleogene Dinarides compressive structures (e.g., Doglioni and Bosellini, 1987; Zanferrari et al., 2013). At the Miocene-Pliocene transition, the counterclockwise rotation of the Adria microplate produced dextral strike-slip deformation in Slovenia (e.g. Marton et al.,

15 2003; Vrabec and Fodor, 2006). Recent activity of dextral strike-slip fault systems is documented by large right-lateral offset of geological and geomorphological features (e.g., Mlakar, 1969; Cunningham et al., 2006, 2007; Moulin et al., 2014, 2016) and by the formation of pull-apart basins (Vrabec, 1994; Kastelic et al., 2008). Seismicity also reflects dextral strike-slip deformation, with major earthquakes having trascurrent focal plane solutions (e.g., Poljak et al., 2010), such as the April 12, 1998 (Mw 5.66) (Bajc et al., 2001; Zupancîč et al., 2001) and July 12, 2004 (Mw 5.1) earthquakes, related to the Ravne

20 strike-slip fault (Kastelic et al., 2008). Quaternary activity of the eastern Southern Alps front is documented by field evidence and seismic lines interpretation (e.g., Zanferrari et al.,1982; Galadini et al., 2005; Zanferrari et al., 2008a-b; Poli et al., 2008; Poli et al., 2009; Zanferrari et al., 2013; Monegato and Poli, 2015), which defined ongoing growth of anticlines on blind active thrusts. The two aforementioned main shocks of the 1976 seismic sequence, in central Friuli, show reverse fault plane solutions, along low angle WNW-ESE to E-W striking and N-dipping reverse faults (Fig. 1a) (Slejko et al., 1999;

25 Pondrelli et al., 2001; Poli et al., 2002), recently confirmed by geodetic data analysis and inversion (Cheloni et al., 2012). Interseismic geodetic data show about 2 mm/yr northwards movement of Adria relative to Eurasia (e.g., D'Agostino et al., 2008; Devoti et al., 2011; Carafa, and Bird, 2016) (Fig. 1a). This is absorbed by WSW-ENE trending, SSE-verging thrust front of the eastern Southern Alps, and by NW-SE trending, right-lateral strike-slip fault systems in western Slovenia. The major historical earthquake of the study area struck on March 1511 (maximum intensity =IX, MCS scale). In spite of many

30 studies, many issues still remain to be solved about this event. Ambraseys (1976) suggested M~6.4 and epicentre located northwest of Tolmin, at the Italy-Slovenia border. Ribaric (1979) suggested that the event have been actually made of two shocks, one occurred at 15h CET in the Idrija zone, in Slovenia, with possible magnitude 6.9, and a second at 20h CET east

of Gemona, in Friuli, with possible magnitude 7.0-7.2. Košir and Cecić (2011) questioned Ribaric's interpretation of the historical information and proposed a single main shock on March 26, at 14:40 GMT. By inverting macroseismic data, Fitzko et al. [2005] hypothesized a possible source of the 1511 earthquake on a 50 km-long segment of the Idrija fault, in Slovenia. The authors proposed NW-ward rupture directivity, with nucleation just to the SE of the Idrija town. This

5 hypothesis is also assumed by the Italian Database of Individual Seismogenic Sources (Basili et al., 2008). Nonetheless, as reported by Fitzko et al. (2005), their model only partly reconciles the actual intensities suffered by many villages in Italy and Slovenia. Indeed, some synthetic intensity data-points differ of up to 2 degrees from the intensities estimated by the historical sources. Moreover, a recent reappraisal of macroseismic data led to a new distribution of intensities (Camassi et al., 2011), where values are strongly decreased in Slovenia. In particular, the intensity of X assigned to Idrija, which was a

10 key point in the Fitzko et al.'s hypothesis, has been removed. Also, Camassi et al. (2011) proposed a new epicenter for the 1511 event in Italy, near Tarcento, and Rovida et al.,(2016) defined Mw 6.3 .

3 Structural observations and seismic line interpretation

The BFCF is a ~25 km-long, N 125°-135° striking dextral strike-slip fault, traceable from Nimis, to the north, to Cividale, to the south (Fig. 1a; 1b) (Moulin et al., 2016). Southwest of the BFCF occurs the CVT, a 10 km-long, WNW-ESE striking

15 thrust. Mesostructural kinematic indicators show a SW-ward vergence (Fig. 1b, inset). The fault front crops out at the base of small reliefs made of early Eocene turbidites (Savorgnano Marls and Arenites) (Zanferrari et al., 2008a) (Fig. 1b), which have been folded and uplifted by the thrust activity. The BFCF and CVT merge towards the SE (Fig. 1b). Interpretation of an industrial seismic line (kindly provided by ENI E&P) allowed us to define the deep geometry of the two structures. The CVT cuts the Quaternary succession (Fig. 1c) and seems to be connected at depth with the BFCF, representing a branching from

20 the same major structure. Two further thrusts (Premariacco thrust and Tarnovo thrust) are also visible in the CVT footwall, deforming the base of the Quaternary. The seismic reflection line also shows the CVT reaching the surface. Moving from this evidence, we focused paleoseismological investigation along the CVT surface trace with the aim of constraining the recent movements of the fault.

4 Morpho-tectonic evidence

25 The sector between the CVT and BFCF is characterized by a low gradient morphology, with flat sectors interposed to small NE-SW elongated gentle reliefs. The streams run from the NE to the SW, and get sinuous entering this low gradient sector. In particular, according to Pascolino (2014) and Moulin et al. (2016), crossing the BFCF, the streams give rise to diversions and deflections indicative of dextral horizontal movements of the strike slip fault (Valle, Poiana and Meris rivers respectively in Fig. 2a)

30 Moving toward the SW (i.e. CVT hanging wall), because of the common water regulations, most of the rivers become rectilinear, getting sinuous again flowing toward the Friulian plain. Such a geomorphic setting suggests the formation of a

low gradient sector at the CVT rear, owing to the progressive growth of the inverse tectonic structure. The presence of two back-tilted surfaces located at the boundary between the Friulian plain and the reliefs (Fig. 2a) corroborates this interpretation.

Moreover, we found remnants of an old paleo-landscape on top of the ridges located between the CVT and BFCF,
5   represented by almost flat landsurfaces carved onto the turbidite bedrock. Interpolation of these top relict landsurfaces (Fig. 2b) indicates NE-wards dipping, that is opposite to the present drainage pattern.

In order to find further evidence of the recent activity of the CVT, we made a core boring 20 m deep just northward of the trenches site (location in Fig. 2a), above an about 5 meters raised fluvial terrace. The borehole (localized at 155 m a.s.l.) found 9 m-thick colluvial sandy silt with thin gravel layers interbedded. Underneath, 6 m-thick grey-blue lacustrine clays
10   was cored. The drilling reached the bedrock (i.e. Savorgnano Marls and Arenites) at 15.40 m depth (Figs. 2c, 3a).

Comparing the depth of bedrock in the trenches (unit 8) with that in the borehole it appears that the Savorgnano Marls and Arenites constitute a morpho-structural high whose progressive growth formed a local depocentre at its back (i.e. a piggy back basin), where a small lacustrine basin constituted by the grey-blue clays (Fig.2c). Within these deposits has been found a wood that has provided an age > 45.000 BP (radiocarbon cal. age, 2σ).

5 Paleoseismological investigations along the CVT

We dug three trenches across a gentle surface scarp (~0.5 m high) seen at the CVT front (Figs. 2a, 3a). The excavations exposed a continental sedimentary sequence, mainly consisting of fluvial and slope deposits that we subdivided into 8 stratigraphic units (Figs. 3, 4; detailed unit description in auxiliary material, Table 1). Chronologic constraints were provided by radiocarbon dating on charcoals found within the units (Table 2 in auxiliary material).

20   The trenches show the whole stratigraphic succession warped (upward convexity) in coincidence with the surface scarp (Figs. 3b, c). The lowermost Units 7 to 4 show a slightly tighter bending than the upper ones (Units 3 to 1). The very localized bending, the coincidence with the surface scarp, and the sedimentological interpretation rule out that this geometrical feature relates to the original depositional attitude of the layers. This is particularly evident for the fluvial Unit 7, whose attitude is expected to be sub-horizontal. Besides this evidence, each excavation showed other features (fractures and
25   shear planes), described below, that can be associated to events of tectonic deformation (Figs. 3b, 3d, 3e, 3f, and 4 a-c).

Trench 1(Figs. 3b and c; Fig. 4a): unit 8 (turbidite bedrock) showed pervasive cleavage with sub-vertical planes about E-W striking, indicative of localized shearing. Slope deposits of Unit 6 is unconformably overlaid by Unit 5. This suggests progressive deformation of the sequence during deposition, with the formation of angular unconformities, i.e. growth strata. Where the sedimentary sequence displayed warping in coincidence with the surface scarp (~0.5 m high), Units 5 and 4 were
30   also displaced by a low angle shear plane. The displacement indicates reverse kinematics, with sense of motion towards the SW (Figs. 3b, 4a). The deformation was also accommodated by a secondary reverse shear plane with opposite sense of displacement. These features were localized where the turbidite bedrock was affected by cleavage, thus demonstrating the presence of a well-developed shear zone active previously.

Trench 2: we identified high angle shear planes that offset Units 4 and 5 with an extensional kinematics, and that were sealed by Unit 3 (Figs. 3d, 4b). The geometrical characteristics of the displaced units and the coincidence with the warped portion of the succession indicate that these shear planes define tension cracking related to bending, interpreted as an extrados-related feature due to a sudden warping event of the paleo-topographic surface. This event occurred after deposition of Unit 4 and before Unit 3.

Trench 3: comparably to trench 2, Units 4 to 6 are disrupted by an extensional fracture which, in turn, was sealed by Unit 3 (Fig. 4c). Moreover, in the easternmost part of the excavation, Unit 6 is brought into lateral contact with Unit 8 (turbidite bedrock) by a sub-vertical shear plane (Figs. 3e, f and 4c). This structural feature is sealed by unit 5. Furthermore, in this sector the basal contact of Unit 5 on the underlying Unit 8 gets slightly convex upward (Fig.3e), suggesting that Unit 5 underwent slight uplift after deposition.

The described evidence allows distinguishing at least three subsequent events of deformation: the oldest event, named E3, is documented by the displacement of Unit 6 along the sub-vertical shear plane which placed it into contact with the bedrock (seen in trench 3) and was sealed by Unit 5. E3 was thus responsible for the first surface faulting. The angular unconformity that separates Unit 5 from Unit 6 (described in trench 1) also supports the occurrence of E3, as Unit 6 has been deformed and tilted towards the SW before the deposition of Unit 5, determining an onlap geometry.

A subsequent event, named E2, is testified by primary and secondary tectonic features, i.e. the reverse fault planes (seen in trench 1), which offset the sequence up to Unit 4, and the extrados fractures (seen in trenches 2 and 3), that developed after Unit 4 deposition and before Unit 3 deposition, respectively. It is worth noting that notwithstanding extrados fractures are secondary surface effects, their formation requires sudden warping. Otherwise, slow and progressive deformation would have been "absorbed" by a continuous deformation of the sediments. The occurrence of E2 is also suggested by the upward bending of Unit 5 overlaying the bedrock (Fig.3e).

The latest event, named E1, is documented by the gentle warping of Units 3 to 1 (seen in all of the trenches), which matches the bending radius of the surface scarp. As units 3–1 display a lower bending than the underlying units 7–4, it testifies that the older units underwent a larger, cumulative deformation produced by E2 + E1.

The radiocarbon ages allow us to constrain E3 before the 5th millennium b.C., based on the ages obtained from charcoals collected within Unit 5, which sealed the event. As for E2 it can be constrained between the 5th and 6th century AD. In particular, charcoals found within Units 4 and 3 – the former displaced by E2 and the latter sealing E2 – provided a radiocarbon age ~6th century AD. This suggests that E2 likely occurred around this period. Lastly, E1 took place after the 15th century AD, based on the youngest radiocarbon age of charcoals found within Unit 2.

6 Discussion and concluding remarks

We performed multiple investigations on the Colle Villano Thrust (CVT) and the Borgo Faris-Cividale strike slip fault (BFCF). These structures located at the intersection between the Slovenian dextral strike-slip active shear zone and the external active thrust front of the eastern Southern Alps. Our main goal was to investigate how active tectonic deformation

distributes in this region of kinematic transition and to improve the seismotectonic knowledge of the area, still incomplete in some important aspects, such as the causative fault of the largest earthquake of the study region, occurred on 1511.

Field observations coupled with the interpretation of a commercial seismic reflection line indicate that the BFCF and CVT gave rise to a major NW-SE-to-WNW-ESE striking transpressive shear zone that accommodates inverse-oblique

5   deformation. This interpretation fits the GPS time series available for the area, which define main N-S trending compression. Therefore, a significant horizontal shear component is inherently expected on a structure obliquely oriented with respect to the N-S trending regional $\sigma 1$, i.e. the axis of maximum compression.

The evidence of active deformation we found along the CVT and the available knowledge on the kinematics of the region suggest that the transpressive slip probably splits on the investigated structures, that is, mainly strike-slip along the BFCF

10   and mainly compressive along the CVT (Fig. 5a and 5b). Slip partitioning on splays of oblique structures has been observed in many cases from across the world, both as for the coseismic and long-term displacements (e.g., Wesnousky and Jones, 1994; Walker et al., 2003; King et al., 2005).

Trench investigations across the CVT attested at least three activation events. The presence of low angle reverse faults, the displacement of some stratigraphic units along sub-vertical shear planes and the occurrence of secondary extrados fractures

15   are indicative of sudden deformation events along the CVT, responsible for primary surface faulting. In detail, chronological data attested the penultimate event E2 likely around the 6th century AD and the last event E1 after the 15th century AD. E1 has been responsible for bending, that caused ~0.5 m high (minimum) surface scarp.

From a seismotectonic viewpoint, the only known post-15th century AD earthquake of the area that has had a magnitude large enough to result in such a significant deformation is that occurred in 1511. In this perspective, basing on the

20   regressions of Wells and Coppersmith (1994), the magnitude of the earthquake, i.e. 6.3 (Camassi et al., 2011; Rovida et al., 2016) is consistent with the activation of the 25 km long CVF-BFCF system. Therefore, the CVT-BFCF system appears as a very plausible candidate for having played a primary role in the seismogenic process of the 1511 seismic event (Fig. 5c). Ultimately, this study raises significant issues on a potential major seismogenic source of a region where interseismic coupling (Cheloni et al., 2014; Serpelloni et al., 2016) suggests tectonic deformation storage as elastic strain at seismogenic

25   depth, available to be released in future large magnitude earthquakes.

Author contribution

Emanuela Falcucci, first and corresponding author, led the paleoseismological investigations, manuscript writing and discussed the seismotectonic interpretation; Eliana Poli and Adriano Zanferrari performed the geological and structural

30   analyses and interpretation of the reflection seismic line; Giancarlo Scardia contributed to the stratigraphic interpretation of the trench walls; Giovanni Paiero contributed to the trenching activity; seismotectonic interpretation was discussed and shared with Fabrizio Galadini. All of the authors discussed the paleoseismological data and general aspects concerning the regional tectonic framework.

Acknowledgments

The study has been funded by the ASSESS project, Regione Friuli Venezia Giulia-Istituto Nazionale di Geofisica e Vulcanologia (INGV) agreement, Project Manager for INGV Dr. Fabrizio Galadini. The borehole was made by means CARG Project funds managed by A. Zanferrari. The authors thank Dr. Stefano Gori for the helpful discussion on active

5   tectonics, structural, and paleoseismological issues and Dr. Andrea, Marchesini for helping us in figures preparation.

References

Ambraseys, N.N.: The Gemona di Friuli earthquake of 6 May 1976, in. In: P. PICHARD a.o. UNESCO, Restricted Technical Report RP/1976–76, 1976.

Bajc, J., Aoudia, A., Sarao, A., and Suhadolc, P.: The 1998 Bovec-Krn mountain (Slovenia) earthquake sequence, Geophys.

10   Res. Lett., 28, 1839-1842, 2001.

Basili, R., Valensise, G., Vannoli, P., Burrato, P., Fracassi, U., Mariano, S., and Tiberti, M.M.: The Database of Individual Seismogenic Sources (DISS), version 3: summarizing 20 years of research on Italy's earthquake geology, Tectonophysics, 453, 20-43, 2008.

Bavec, M., Atanackov, J., Celarc, B., Hajdas, I., Jamšek Rupnik, P., Jež, J., Kastelic, V., Milanič, B., Novak, M., Skaberne,

15   D. and Žibret, G.: Evidence of Idrija fault seismogenic activity during the Late Holocene including the 1511 Mm 6.8 earthquake, Proceedings of the 4th International INQUA Meeting on Paleoseismology, Active Tectonics and Archeoseismology (PATA), 9-14 October 2013, Aachen, Germany, 2013.

Bernardis, G., Poli, M.E., Snidarcig, A., and Zanferrari, A.: Seismotectonic and macroseismic characteristics of the earthquake of Bovec (NW Slovenia: April 12, 1998), Bollettino di Geofisica Teorica ed Applicata, 41(2), 133-148, 2000.

20   Camassi, R., Caracciolo, C.H., Castelli, V., and Slejko, D.: The 1511 Eastern Alps earthquakes: a critical update and comparison of existing macroseismic datasets, J. Seismol., 15, 191-213, 2011.

Carafa, M.M.C., and Bird, P.: Improving deformation models by discounting transient signals in geodetic data, 2: Geodetic data, stress directions, and long-term strain rates in Italy, J. Geophys. Res., 121(7), 5557-5575, doi: 10.1002/2016JB013038, 2016.

25   Carulli, G.B.: Carta geologica del Friuli Venezia Giulia alla scala 1:150.000. Regione Autonoma Friuli Venezia Giulia, Direzione Centrale Ambiente e Lavori Pubblici, Servizio Geologico. SELCA Firenze, 2006.

Castellarin, A., Nicolich, R., Fantoni, R., Cantelli, L., Sella, M., and Selli, L.: Structure of the lithosphere beneath the Eastern Alps (southern sector of the TRANSALP transect), Tectonophysics, 414, 259–282, 2006.

Cheloni, D., D'Agostino, N., and Selvaggi, G.: Interseismic coupling, seismic potential and earthquake recurrence on the southern front of the Eastern Alps (NE Italy), J. Geophys. Res. Solid Earth, 119, 4448-4468, doi:10.1002/2014JB010954, 2014.

Cheloni, D., D'Agostino, N., D'Anastasio, E., and Selvaggi, G.: Reassessment of the source of the 1976 Friuli, NE Italy, earthquake sequence from the joint inversion of high-precision levelling and triangulation data, Geophys. J. Int., 190, 1279–1294, doi:10.1111/j.1365-246X.2012.05561.x, 2012.

Cunningham, D. Grebby, S., Tansey, K., Gosar, A., and Kastelic, V.: Application of airborne LiDAR to mapping seismogenic faults in forested mountainous terrain, southeastern Alps, Slovenia, Geoph. Res. Lett., 33, L20308, doi: 0.10/29/2006GL027014, 2006.

Cunningham, D. Gosar, A. Kastelic, V. Grebby, S., and Tansey, K.: Multi-disciplinary investigations of active faults in the Julian Alps, Slovenia, Acta Geodyn. Geomater., 4(1), 77-85, 2007.

D'Agostino, N., Avallone, A., Cheloni, D., D'Anastasio, E., Mantenuto, S., and Selvaggi, G.: Active tectonics of the Adriatic region from GPS and earthquake slip vectors, J. Geoph. Res., 113, B12413, doi:10.1029/2008JB005860, 2008.

Devoti, R., Esposito, A., Pietrantonio, G., Pisani, A.R., and Riguzzi, F.: Evidence of large scale deformation patterns from GPS data in the Italian subduction boundary, Earth and Planetary Science Letters, 311, 230-241, 2011.

Doglioni, C,. and Bosellini, A.: Eoalpine and mesoalpine tectonics in the Southern Alps, Geol. Rundsch., 76, 735-754, 1987.

Fitzko, F., Suhadolc, P., Aoudia, A., and Panza, G.F.: Constrains on the location and mechanism of the 1511 Western-Slovenia earthquake from active tectonics and modeling of macroseismic data, Tectonophysis, 404, 77-90, 2005.

Galadini, F., Poli, M.E., and Zanferrari, A.: Seismogenic sources potentially responsible for earthquakes with M ≥ 6 in the eastern Southern Alps (Thiene-Udine sector, NE Italy), Geophys. J. Int., 161, 739-762. doi: 10.1111/j.1365-246X.2005.02571.x, 2005.

Kastelic, V., Vrabec, M., Cunningam, D., and Gosar, A.: Neo-Alpine structural evolution and present day tectonic activity of the eastern Southern Alps: the case of the Ravne fault, NW Slovenia, J. Structural Geol., 30, 963-965, 2008.

King, G., Klinger, Y., Bowman, D., and Tapponier, P.: Slip-partitioned surface break for the Mw 7.8 2001 Kokoxili earthquake, China, Bull. Seism. Soc. Am., 95, 731-738, 2005.

Košir, M., and Cecić I.: Potres 26. marca 1511 v luči novih raziskav. Idrijski razgledi, 56/1, pp. 90–104, 2011.

Locati, M., Camassi, R., Rovida, A., Ercolani, E., Bernardini, F., Castelli, V., Caracciolo, C.H., Tertulliani, A., Rossi, A., Azzaro, R., D'Amico, S., Conte, S., and Rocchetti, E.: DBMI15, the 2015 version of the Italian Macroseismic Database. Istituto Nazionale di Geofisica e Vulcanologia. doi:http://doi.org/10.6092/INGV.IT-DBMI15, 2016

Marton, E., Drobne K., Cosovic V., and Moro, A.: Palaeomagnetic evidence of Tertiary counterclockwise rotation of Adria. Tectonophysiscs, 377, 143-156, 2003.

Mlakar, I.: Krovna zgradba idrijsko Zirovskega ozamlja, Geologija 12, 5-72, 1969

Monegato, G., and Poli, M.E.: Tectonic and climatic inferences from the terrace staircase in the Meduna valley, eastern
5 Southern Alps, NE Italy, Quaternary Research, 83, 229-242, 2015.

Moulin, A., Benedetti, L., Rizza, M., Rupnik, P.J., Gosar, A., Bourlès, D.: The Dinaric fault system: Large-scale structure,
rates of slip, and Plio-Pleistocene evolution of the transpressive northeastern boundary of the Adria microplate, Tectonics 35
(10), 2258-2292, 2016.

Pascolino, M.: Analisi morfotettonica dei rilievi collinari compresi tra il Torrente Malina (Attimis) e il Torrente Grivò
10 (Faedis), Unpublished MS Thesis, Scienze per l'Ambiente e la Natura, Università degli Studi di Udine, 2014.

Placer, L, Vrabec M., and Ceralac, B.: The bases for understanding of the NW Dinarides and Istria Peninsula tectonics
Geologija 53/1, 55-86, Ljubljana, 2010.

Poli, M.E., Zanferrari A., and Monegato, G.: Geometria, cinematica e attività pliocenico-quaternaria del sistema di
sovrascorrimenti Arba-Ragogna (Alpi Meridionali orientali, Italia NE), Rendiconti online Soc. Geol. It., 5, 172-175, 2009.

15 Poli, M.E., Burrato, P., Galadini, F., and Zanferrari, A.: Seismogenic sources responsible for destructive earthquakes in NE
Italy. Boll. Geof. Teor. Appl., 49, 301-313, 2008.

Poli, M. E., Peruzza, L., Rebez, A., Renner, G., Slejko, D., and Zanferrari, A.: New seismotectonic evidence from analysis of
the 1976-1977 and 1977-1999 seismicity in Friuli (NE Italy), Boll. Geof. Teor. Appl., 43, 1-2, 53-78, 2002.

Poljak, M., Gosar, A., and Živcič, M.: Active tectonics in Slovenia. In: Geology of Adriatic Area, Geo Acta Special
20 Pubblication, 3, 15-24, 2010.

Pondrelli, S., Ekstro, G., and Morelli, A.: Seismotectonic re-evaluation of the 1976 Friuli, Italy, seismic sequence, J. Seism.,
5, 73–83, 2001.

Ribaric, V.: The Idrija earthquake of March 26, 1511 a reconstruction of some seismological parameters, Tectonophysics,
53, 315-324, 1979.

25 Serpelloni, E., Vannucci, G. Anderlini, L. and Bennett, R. A.: Kinematics, seismotectonics and seismic potential of the
eastern sector of the European Alps from GPS and seismic deformation data, Tectonophysics, 688, doi:
10.1016/j.tecto.2016.09.026, 2016.

Slejko, D., Camassi, R., Cecić, I., Herak, D., Herak, M., Kociu, S., Kouskouna, V., Lapajne, J., Makropoulos, K., Meletti, C., Muço, B., Papaioannou, C., Peruzza, L., Rebez, A., Scandone, P., Sulstarova, E., Voulgaris, N., Zîvčić, M. and Zupancîč, P.: Seismic hazard assessment for Adria, Annals of Geophysics, 42, 1085-1107, 1999.

Vrabec, M.: Some thoughts on the pull-apart origin of karst poljes along the Idrija strike slip fault in Slovenia, Acta
5 Carseologica, XXIII, 155-167, Liubljana, 1994.

Vrabec, M., and Fodor, L.: Late Cenozoic tectonics of Slovenia: Structural styles at the northeastern corner of the Adriatic microplate, in: Pinter N., Grenerczy Gy., Weber J., Stein S. & Medak D. (Eds.): The Adria microplate: GPS geodesy, tectonics, and hazards. Springer, 151-168, 2006.

Walker, R., Jackson, J., and Baker, C.: Surface expression of thrust faulting in eastern Iran: source parameters and surface
10 deformation of the 1978 Tabas and 1968 Ferdows earthquake sequences, Geophys. J. Int., 152, 749-765, 2003.

Wells, D. L., and Coppersmith, K. J.: Analysis of empirical relationships among magnitude, rupture length, rupture area, and surface displacement, Bulletin of the Seismological Society of America, 84, 974-1002, 1994.

Wesnousky, S.G., and Jones, C.H.: Oblique slip, slip partitioning, spatial and temporal changes in the regional stress field, and relative strength of active faults in the Basin and Range, western United States, Geology, 22, 1031-1034, 1994.

15 Zanferrari, A., Bollettinari, G., Carobene, L., Carton, A., Carulli, G.B., Castaldini, D., Cavallin, A., Panizza, M., Pellegrini, G.B., Pianetti, F., and Sauro, U.: Evoluzione neotettonica dell'Italia nord-orientale. Mem. Sci. Geol.., 35, 355-376, Padova, 1982.

Zanferrari, A., Avigliano, R., Monegato, G., Paiero, G., Poli, M.E., and Stefani, C.: Geological map and explanatory notes of the Geological Map of Italy at the scale 1:50.000: Sheet 066 "Udine". APAT-Servizio Geologico d'Italia – Regione
20 Autonoma Friuli Venezia Giulia, 176 pp. http://www.isprambiente.gov.it/Media/carg/friuli.html, 2008a

Zanferrari, A., Avigliano, R., Grandesso, P., Monegato, G., Paiero, G., Poli, M.E., and Stefani, C.: Geological map and explanatory notes of the Italian Geological Map at the scale 1:50.000: Sheet 065 "Maniago". APAT-Servizio Geologico d'Italia – Regione Autonoma Friuli Venezia Giulia. http://www.isprambiente.gov.it/Media/carg/friuli.html, 2008b.

Zanferrari, A., Masetti, D., Monegato, G., and Poli, M.E.: Geological map and explanatory notes of the Geological Map of
25 Italy at the scale 1:50.000: Sheet 049 "Gemona del Friuli". ISPRA - Servizio Geologico d'Italia - Regione Autonoma Friuli Venezia Giulia, 262 pp. http://www.isprambiente.gov.it/Media/carg/friuli.html, 2013.

Zupancîč, P., Cecić I., Gosar A., Placer, L., Poljak, M., and Zîvčić, M.: The earthquake of 12 April 1998 in the Krn Mountains (Upper Soča valley, Slovenia) and its seismotectonic characteristics. Geologija 44 (1), 169–192, 2001.

30
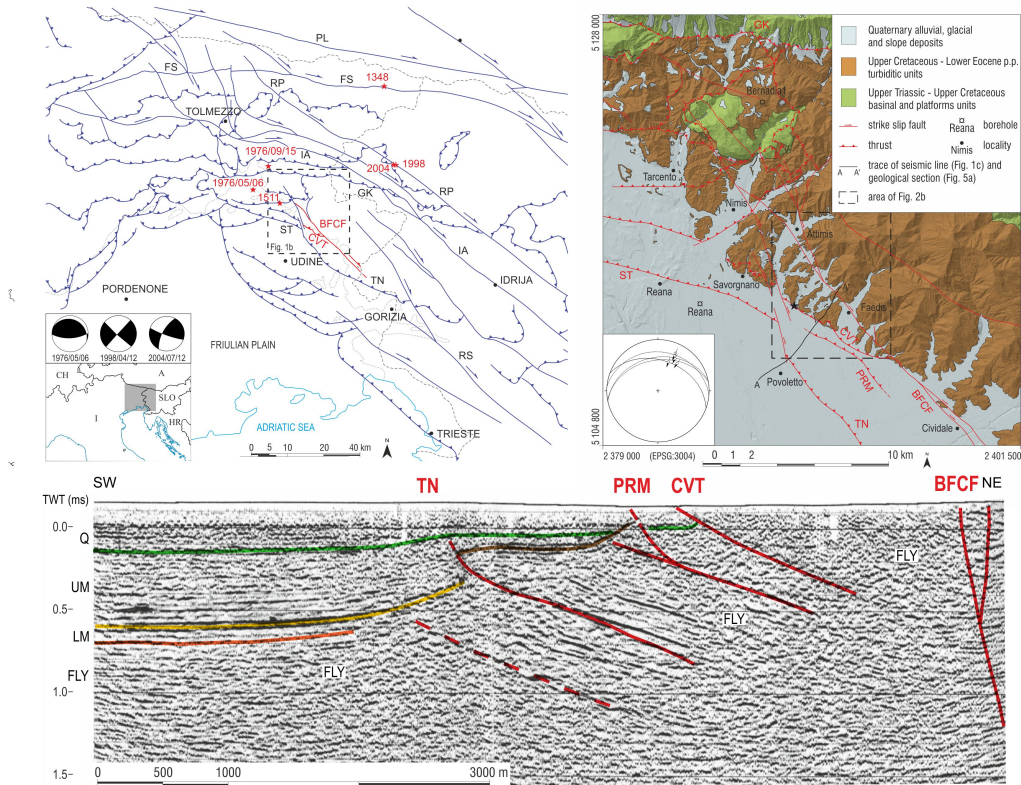
Figure 1: a) Tectonic map of the eastern Southern Alps and western Dinarides (modified from Zanferrari et al., 2013). Adria CCW rotation (D'Agostino et al., 2008), inset, BFCF: Borgo Faris – Cividale fault; CVT: Colle Villano thrust; GK: Gemona-Kobarid thrust; IA: Idrija-Ampezzo fault; Periadriatic lineament; RP: Ravne-Paularo fault; RS: Raša fault ; ST: Susans-Tricesimo thrust; TN: Tarnovo nappe thrust front [*Placer et al.,* 2010]. Red stars: epicentres of the strongest historical and instrumental earthquakes
5 **[*Rovida et al.,* 2016] and the related focal plane solutions. Italian boundary, thin dashed line. Hills-plain boundary, dotted lines. b) Geological map of the study area (modified from *Carulli, 2006; Zanferrari et al., 2008a; 2013*). PRM: Premariacco thrust. Paleoseimological trenches site, black star. Stereographic projection (lowe hemisphere) of striations collected on the CVT, inset. c) Interpretation of the reflection seismic section (A-A' in Fig. 1b). Q: Quaternary; UM: Middle-Upper Miocene Molasse; LM: Cavanella Group (Lower-Middle Miocene); FLY: Upper Cretaceous-Lower Eocene p.p. turbiditic units.**
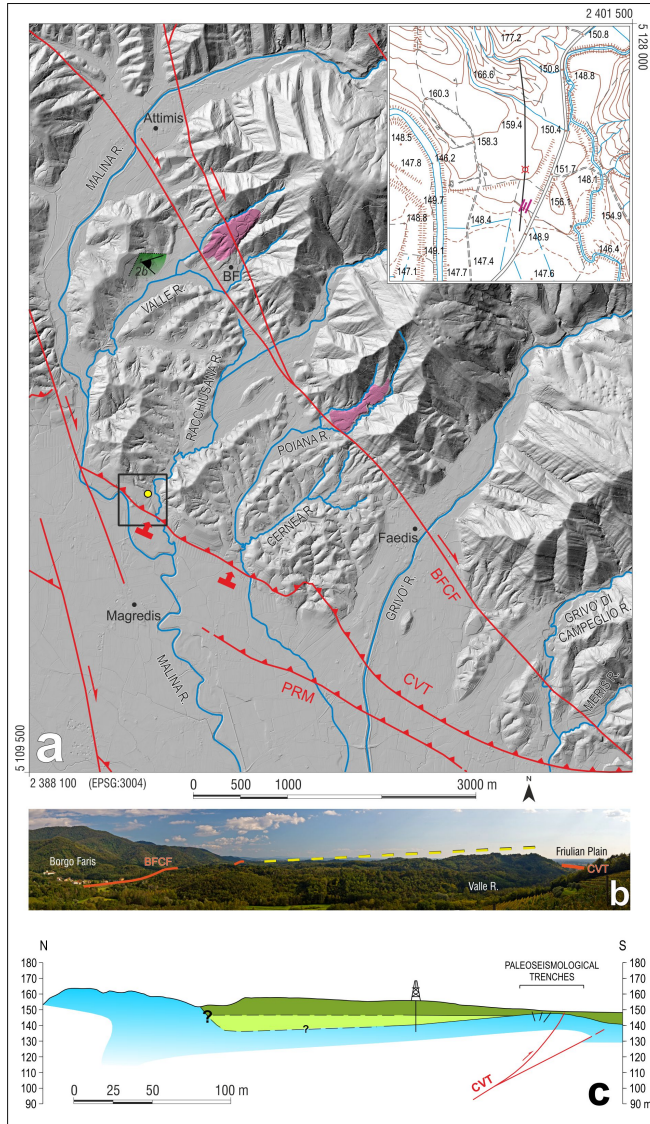
Figure 2: (a) Digital Elevation Model of the study area. Faults: BFCF; CVT; PRM, Premariacco thrust; BF: Borgo Faris village. Back-tilted surfaces at the Racchiusana and Poiana valleys outlet, red arrows. In pink the two suspended glacis cut off by the BFCF. Site of the paleoseismological trenches, black square; site of the core logging, yellow dot. (b) The NE dipping paleolandscape carved in the turbidite bedrock (yellow dotted line) between the BFCF and the CVT. Point of view in Figure 2a (green eye). (c) Geological section across the core logging and the paleoseismological trenches. The light green lacustrine clay

doesn't crop out in the trenches but on-laps the growing anticline built in the turbiditic bedrock (light blue). Dark green: alluvial and colluvial deposits.
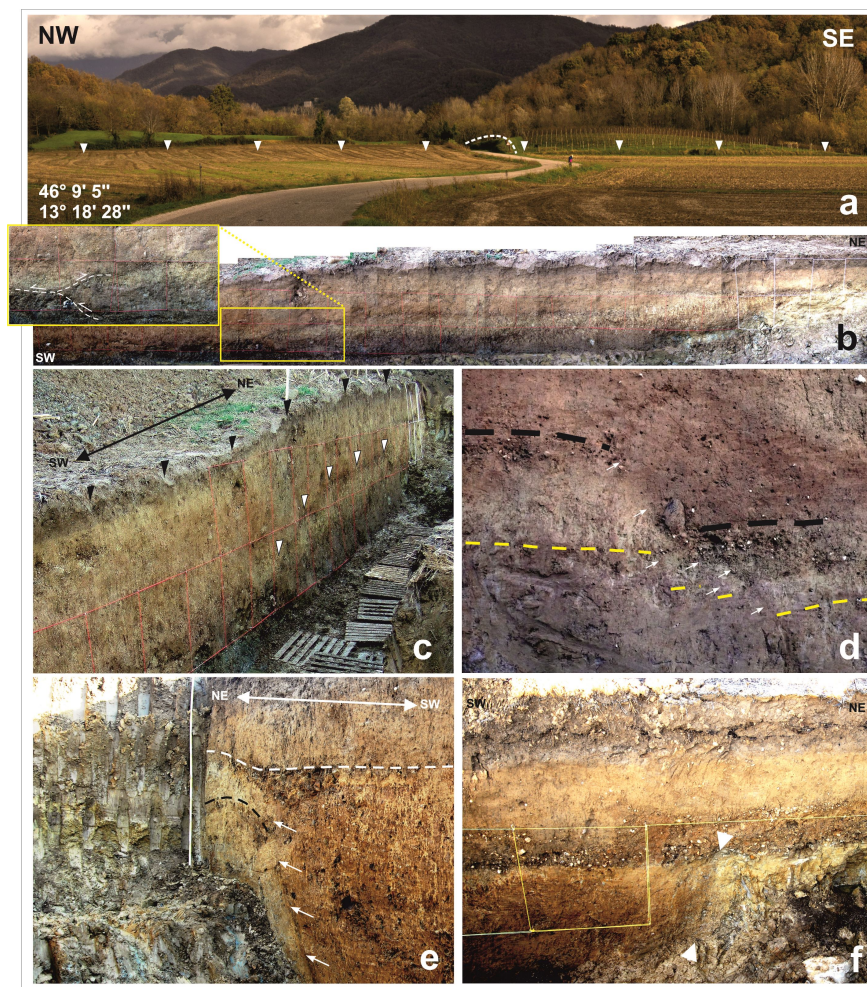
Figure 3: a) Racchiusana valley outlet, north of Magredis. Trenches location, black rectangle. (b) Trench 1, northern wall; reverse fault planes (white dashed lines in inset). (c) Trench 1, northern wall; bending (marked by white triangles) of the stratigraphic units in coincidence with the surface scarp (black triangles). (d) Trench 2, southern wall; fracture planes (indicated by white arrows) displacing the units (attitude marked by black and yellow dashed lines. (e) Trench 3, southern wall; shear plane (white

10.5194/se-2017-131
2018-01-02
Author(s) 2018

arrows) displacing the upward warped stratigraphic units (black and white dashed lines). (f) Trench 3, northern wall, high angle shear plane (white arrows) placing into contact the bedrock (unit 8) with the late Quaternary units.
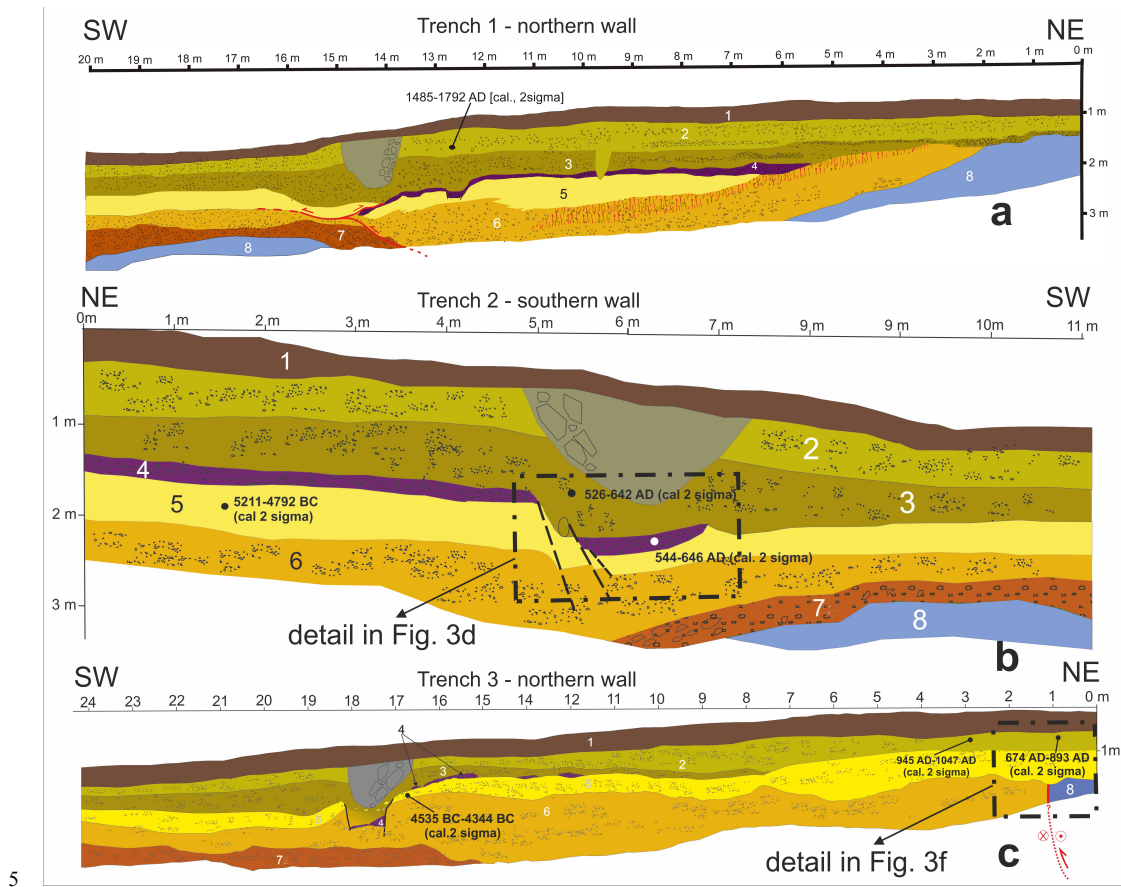
Figure 4: rench walls, stratigraphic schemes. Units: 1, soil; 2, 3, 5 and 6, colluvial deposits; 4 and 7, fluvial deposits; 8, turbiditic bedrock.
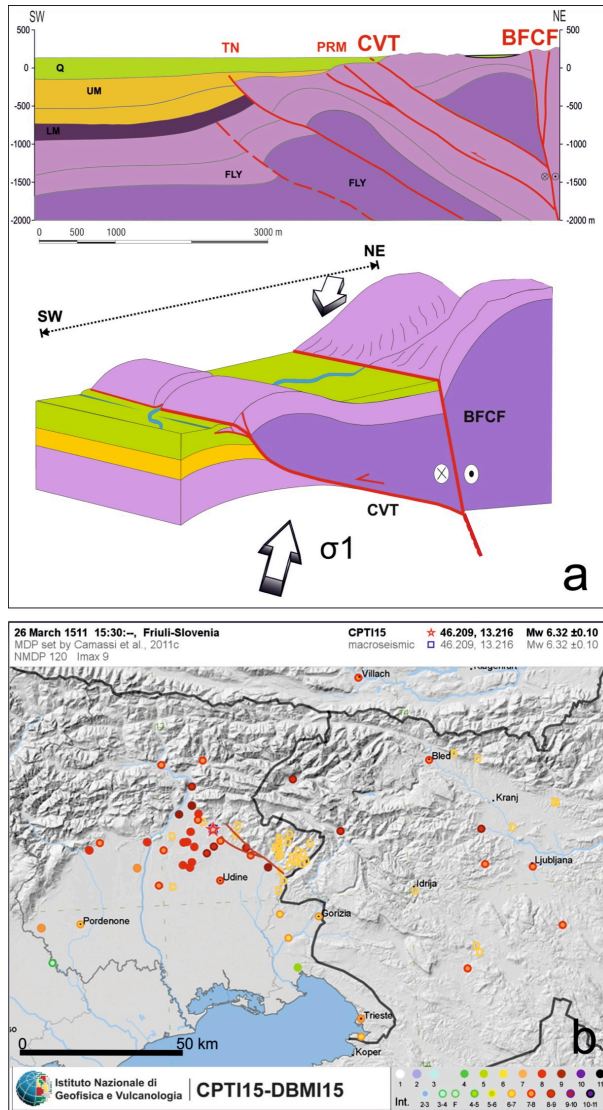
Figure 5: a) Geological cross section based on the seismic line of Figure 1c (AA' in Figure 1b) and 3-D scheme (lower panel) of the BFCF-CVT system. Q: Quaternary; UM: Middle-Upper Miocene Molasse; LM: Cavanella Group (Lower-Middle Miocene); FLY:
5 Upper Cretaceous – Lower Eocene turbiditic sequence. TN: Tarnovo Nappe front (according to Placer et al., 2010); (b) damage distribution of the 1511 earthquake (Rovida et al., 2016); red lines, BFCF-CVT system.